Available online at www.sciencedirect.com

ScienceDirect

journal homepage: www.elsevier.com/locate/issn/15375110

Special Issue: Irrigated Agriculture

Research Paper

Satellite-based evapotranspiration of a super-intensive olive orchard: Application of METRIC algorithms

Isabel Pôças [a,b,*], Teresa A. Paço [a], Mário Cunha [b,c], José A. Andrade [d], José Silvestre [a,e], Adélia Sousa [d], Francisco L. Santos [d], Luís S. Pereira [a], Richard G. Allen [f]

[a] CEER Biosystems Engineering, Instituto Superior de Agronomia, Universidade de Lisboa, Tapada da Ajuda, 1349-017 Lisboa, Portugal
[b] Centro de Investigação em Ciências Geo-Espaciais (CICGE), Porto, Portugal
[c] Faculdade de Ciências da Universidade do Porto, Porto, Portugal
[d] ICAAM, Instituto de Ciências Agrárias e Ambientais Mediterrânicas, Universidade de Évora, Évora, Portugal
[e] Instituto Nacional de Investigação Agrária e Veterinária, Dois Portos, Portugal
[f] University of Idaho, Research and Extension Center, Kimberly, Idaho, USA

ARTICLE INFO

Article history:
Published online 16 July 2014

Keywords:
Landsat images
Leaf area index
Momentum roughness length
Remote sensing
Surface energy balance
Surface temperature

METRIC™ is a satellite-based surface energy balance model aimed at estimating and mapping crop evapotranspiration (ET). It has been applied to a large range of vegetation types, mostly annual crops. When applied to anisotropic woody canopies, such as olive orchards, extensions are required to algorithms for estimating the leaf area index (LAI), surface temperature, and momentum roughness length (Z_{om}). The computation of the radiometric surface temperature needs to consider a three-source condition, thus differentiating the temperature of the canopy (T_c), of the shaded ground surface (T_{shadow}), and of the sunlit ground surface (T_{sunlit}). The estimation of the Z_{om} for tall and incomplete cover is based upon the LAI and crop height using the Perrier equation. The LAI, Z_{om}, and temperature derived from METRIC after these adjustments were tested against field collected data with good results. The application of METRIC to a two year set of Landsat images to estimate ET of a super-intensive olive orchard in Southern Portugal produced good ET estimates that compared well with ground-based ET. The analysis of METRIC performance showed a quantitative improvement of ET estimates when applying the three-source condition for temperature estimation, as well as the Z_{om} computation with the Perrier equation. Results show that METRIC can be used operationally to estimate and mapping ET of super-intensive olive orchards aiming at improving irrigation water use and management.

* *Corresponding author*. CEER Biosystems Engineering, Instituto Superior de Agronomia, Tapada da Ajuda, 1349-017 Lisboa, Portugal. Tel.: +351220402160.
E-mail addresses: ipocas@mail.icav.up.pt, isabel.pocas@fc.up.pt (I. Pôças).
http://dx.doi.org/10.1016/j.biosystemseng.2014.06.019
1537-5110/

Symbols and abbreviations

Nomenclature

a	adjustment factor for the distribution of leaf area index within the canopy [ ]
ALEXI	Atmosphere–Land Exchange Inverse
CIMEC	Calibration using Inverse Modelling at Extreme Conditions
D	ratio of vegetation height vs. width [ ]
DOY	Day of the year [ ]
d	zero plane displacement height [m]
dT	near surface air temperature difference [K]
E_s	soil evaporation [mm d^{-1}]
$E_{s\ sim}$	Soil evaporation modelled by SIMDualKc [mm d^{-1}]
ET	actual evapotranspiration [mm d^{-1}]
ET_{ec}	evapotranspiration obtained by Eddy Covariance technique [mm d^{-1}]
ET_{inst}	instantaneous evapotranspiration [mm h^{-1}]
ET_{METRIC}	evapotranspiration estimated by METRIC [mm d^{-1}]
ET_{obs}	evapotranspiration derived from field observations [mm d^{-1}]
ET_r	Alfalfa reference evapotranspiration [mm d^{-1}]
ETrF	fraction of reference evapotranspiration [ ]
$ETrF_{inst}$	instantaneous fraction of reference evapotranspiration [ ]
ETM+	Enhanced Thematic Mapper Plus
F_{LAI}	proportion of leaf area index lying above $h/2$ [ ]
f_{bl}	Factor describing the proportion of bottom leafless portion of the tree and not casting a shadow due to the total height of the tree [ ]
f_c	fraction of ground covered by vegetation, when viewed from nadir [ ]
$f_{nonvisible}$	Fraction of the canopy that has a shadow under it which is not visible from the satellite [ ]
f_{shadow}	Fraction of ground covered by shadow, when viewed from nadir [ ]
f_{shape}	factor to adjust for differences in shape between trees and their shadow when viewed from nadir [ ]
f_{stot}	fractional area covered by a shadow cast by the crowns [ ]
f_{sunlit}	fraction of ground covered by sunlit, when viewed from nadir [ ]
f_w	fraction of ground wetted [ ]
G	soil heat flux [W m^{-2}]
H	sensible heat flux [W m^{-2}]
h	crop height [m]
IR	infrared
K	Extinction coefficient [ ]
K_c	Crop coefficient [ ]
K_{cb}	Basal crop coefficient [ ]
K_e	Soil evaporation coefficient [ ]
K_{cr}	Alfalfa crop coefficient [ ]
LAI	Leaf Area Index [m^2 m^{-2}]
METRIC™	Mapping EvapoTranspiration at high Resolution using Internalised Calibration
NDVI	Normalised Difference Vegetation Index [ ]
PAR	Photosynthetically Active Radiation
Q_i	daily PAR measured at the top of the canopy [μmol m^{-2}]
Q_0	daily PAR measured below the canopy [μmol m^{-2}]
$r_{ah1,2}$	aerodynamic resistance to heat transport between two heights [s m^{-1}]
R_n	net radiation [W m^{-2}]
SAVI	Soil Adjusted Vegetation Index [ ]
SEBAL	Surface Energy Balance Algorithm for Land
T_c	temperature of the canopy [K]
$T_{c,METRIC}$	average temperature estimated with METRIC [K]
$T_{c,ground\ data}$	ground-based temperature [K]
$T_{coldpixel}$	temperature of the cold pixel [K]
$T_{hotpixel}$	temperature of the hot pixel [K]
TM	Thematic Mapper
T_s	surface temperature [K]
TSEB	Two-Source Energy Balance
T_{sf}	Plant transpiration [mm d^{-1}]
T_{shadow}	temperature of the shaded ground surface [K]
T_{sunlit}	temperature of the sunlit ground surface [K]
$T_{wetbulb}$	temperature of the wet bulb [K]
VI	Vegetation index [ ]
w	vegetation width [m]
Z_{om}	momentum roughness length [m]
λ	latent heat of vaporisation [J kg^{-1}]
λE	latent heat flux [W m^{-2}]
θ	sun zenith angle [rad]

1. Introduction

The intensification of irrigated agriculture leads to the need to improve irrigation management and adopt sustainable irrigation practices. These issues are particularly relevant in the Mediterranean regions, where water scarcity problems are rising. In recent years, many olive orchards, which are a major crop in the Mediterranean agricultural systems, have been converted into intensive or super-intensive hedgerow systems, with very high plant density and irrigation (Orgaz, Testi, Villalobos, & Fereres, 2006; Testi, Villalobos, & Orgaz, 2004; Testi, Villalobos, Orgaz, & Fereres, 2006). Therefore, the accurate estimation of crop water requirements, i.e., crop evapotranspiration (ET), and its spatio-temporal variability at field level is an increasingly important issue for optimising water management.

In recent decades, remote sensing-based techniques have been used for irrigation water management (e.g., Calera, Jochum, García, Rodríguez, & Fuster, 2005; D'Urso et al., 2010). The synoptic and repetitive coverage of Earth Observation data with high spatial resolution makes this type of data interesting for monitoring and quantifying the spatial and temporal variation of ET. The most widely used remote

sensing applications for ET mapping use vegetation index (VI) approaches or surface energy balance models based on thermal-infrared data. The first approach considers the relationships between VI derived from remotely sensed reflectance data and crop coefficients (K_c), considering both single and dual K_c approaches for the estimation of crop ET (Allen, Pereira, Raes, & Smith, 1998). In the single approach both crop transpiration and soil evaporation are time-averaged and integrated into a single coefficient, whereas in the dual approach a basal crop coefficient (K_{cb}), representing primarily the plant transpiration component of ET, and a soil evaporation coefficient (K_e) are considered separately. Several studies documented in the literature report the relationships for different crop types between VI and K_{cb} (e.g., Calera et al., 2005; Campos, Neale, Calera, Balbontín, & González-Piqueras, 2010; Jayanthi, Neale, & Wright, 2007) and between VI and K_c (e.g., Garatuza-Payan & Watts, 2005; Heilman, Heilman, & Moore, 1982).

Satellite-based surface energy balance models have been successfully applied to estimate and map actual crop ET. Examples of such models include METRIC™, Mapping Evapo-Transpiration at high Resolution using Internalised Calibration (Allen, Tasumi, & Trezza, 2007), originated from SEBAL – Surface Energy Balance Algorithm for Land (Bastiaanssen, Menenti, Feddes, & Holtslag, 1998), and TSEB – Two-Source Energy Balance (Kustas, Norman, Schmugge, & Anderson, 2004). These models estimate the ET flux for each pixel of a satellite image (containing both short wave and thermal information) as a "residual" component of the surface energy balance at the time of satellite overpass, i.e., by subtracting the soil heat flux (G) and sensible heat flux (H) from the net radiation (R_n) at the surface.

METRIC and SEBAL are both one-source models, i.e., they consider soil and vegetation as a sole source, whereas TSEB is a two-source model for heat transfer where soil and vegetation areas are partitioned according to vegetation indices. METRIC and SEBAL use a CIMEC process (Calibration using Inverse Modelling at Extreme Conditions) to remove effects of biases in surface temperature (T_s), atmospheric correction of reflectance, and estimation of sensible heat flux, while TSEB follows a more direct approach to the surface energy balance (Anderson, Allen, Morse, & Kustas, 2012). In general, TSEB performs best when air temperature fields are known and T_s data are highly accurate, or when an atmospheric boundary layer condition is input as done in ALEXI (Atmosphere–Land Exchange Inverse) applications (Anderson, Kustas, & Norman, 2003, 2012). However, the data required to parameterise and apply TSEB and ALEXI are often not readily available as in the case of this study. The current study focuses on applying the METRIC algorithm, which has been used over a large range of vegetation types and applications (Allen, Tasumi, Morse et al., 2007; Anderson et al., 2012; Póças, Cunha, Pereira, & Allen, 2013; Tasumi & Allen, 2007) including traditional olive orchards (Santos, Lorite, Allen, & Tasumi, 2012).

In the application of the single-layer-blended METRIC model to sparse woody canopies, some extensions related to the estimation of vegetation temperature in tall canopies and the estimation of momentum roughness length (Z_{om}) and sensible heat flux for tall vegetation must be considered and tested. In such types of crops, having discontinuous ground cover, the pixel temperature observed by satellite integrates a mixture of the temperatures of different surfaces, i.e, sunlit and shaded canopy surfaces, along with sunlit and shaded soil surfaces, which may create biases in the estimation of H. To avoid or minimise such impacts, the computation of the radiometric temperature T_s should consider a three-source condition, allowing the differentiation of the temperature of each one of those surfaces (Allen & Kjaersgaard, 2009). Furthermore, the computation of H may be biased by uncertainties in the definition of Z_{om}, which is a measure of the form drag and skin friction for the layer of air that interacts with the surface (Allen, Trezza, Tasumi, & Kjaersgaard, 2012). For tall vegetation, Z_{om} increases with the orchard density until a threshold density is reached, which occurs for a density corresponding to LAI values around 3 m^2 m^{-2} when trees have a more uniform distribution of the leaves in the canopy (Allen et al., 2012). At this threshold, the density of the orchard becomes high enough to bring the zero plane displacement height (d) upwards to the top of the canopy and Z_{om} reduces for densities above that limit (Allen et al., 2012; ASCE, 1996, pp. 125–252). Therefore, such an effect must be considered in the estimation of Z_{om} in discontinuous woody crops, such as in super-intensive olive orchards.

The current study aims to estimate ET for different stages of the growing season in a super-intensive olive orchard in Southern Portugal and, therefore, find appropriate solutions for the parameterisation of the METRIC model, which was not previously applied to these dense canopies. Specific objectives include testing and evaluating the performance of the adjustments applied for parameterisation of the METRIC algorithm to estimate ET for these orchards, more specifically relative to estimating LAI, the surface temperature and the momentum roughness length, as well as to assess these improvements through comparing the corresponding estimates with field observed data.

2. Material and methods

2.1. Study area

The study area is located in a commercial super-intensive olive orchard in Viana do Alentejo, in Southern Portugal (38°24′N, 7°43′ W, 143 m a.s.l.; Fig. 1). The olive orchard occupies a total area of around 78 ha, with an undulating terrain. The climate is Mediterranean, of type *Csa* according to the Köppen classification (McKnight & Hess, 2000, pp. 205–211). A brief summary of the temperatures, precipitation and alfalfa reference ET (ET_r) in the study (2011 and 2012) is presented in Table 1. The dominant winds blow from the quadrant between N and W.

The olive orchard was planted in 2006 adopting a hedgerow system with 1.35 m × 3.75 m spacing, thus with high tree density (1975 trees ha^{-1}), and an orientation South–North. The olive trees are of cultivar Arbequina and their height is around 3.5 m. The fraction of ground covered by the vegetation (f_c) was approximately 0.35. Soils are sandy loam, with soil water content averaging 0.24 cm^3 cm^{-3} at field capacity and 0.12 cm^3 cm^{-3} at the wilting point.

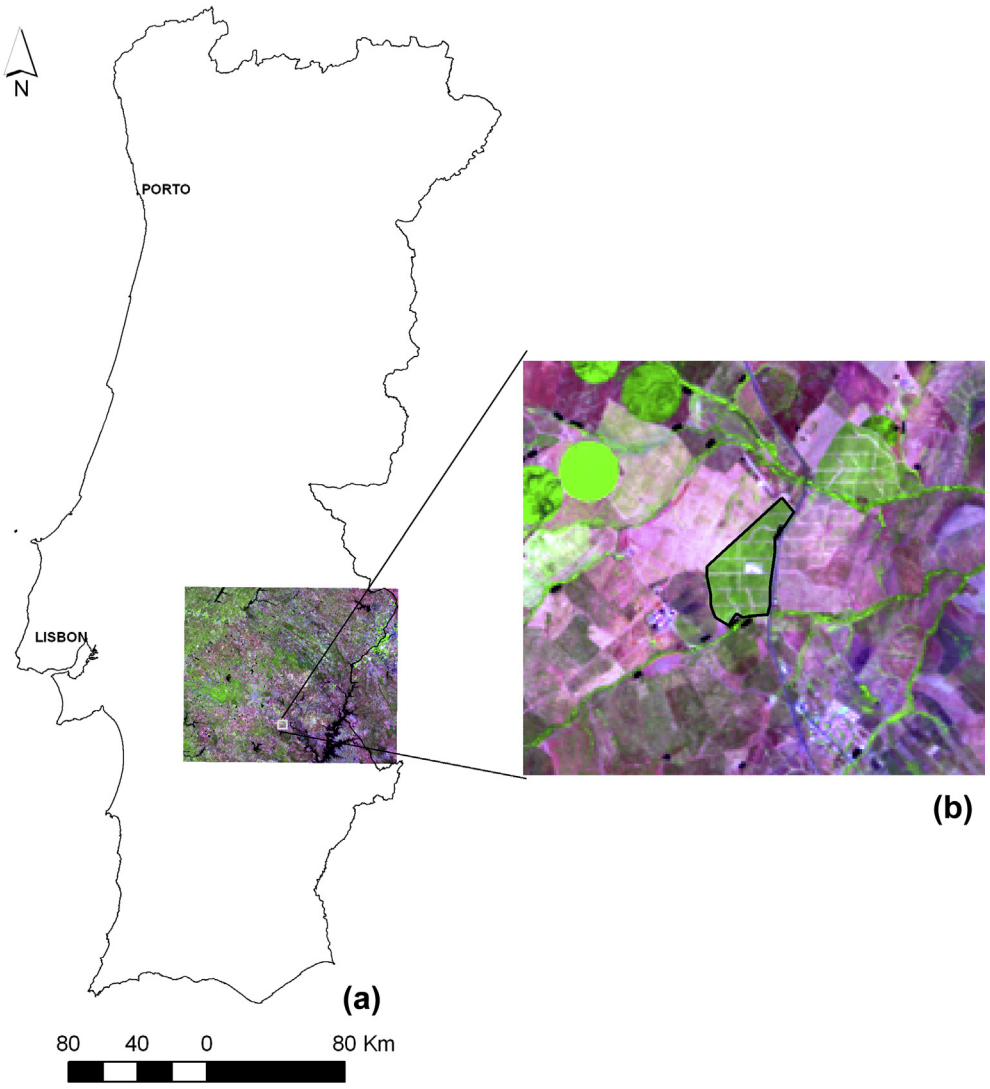

Fig. 1 – Location of the study area in southern Portugal (a), with the identification of the super-intensive olive orchard in the Landsat image (b) (scene 203/033; RGB combination 5:4:3).

Table 1 – Summary of the monthly values of mean daily maximum and mean daily minimum temperatures [°C], precipitation [mm month^{-1}] and alfalfa reference evapotranspiration [ET_r; mm month^{-1}], for the studied years.

Month	Mean daily maximum temperature [°C]		Mean daily minimum temperature [°C]		Precipitation [mm month^{-1}]		ET_r [mm month^{-1}]	
	2011	2012	2011	2012	2011	2012	2011	2012
January	14.1	15.8	5.4	2.8	76.1	15.0	36.7	47.2
February	17.1	16.0	4.8	0.0	62.5	0.6	59.3	83.0
March	17.9	21.3	6.5	5.7	39.3	25.1	86.2	129.1
April	24.6	18.0	10.7	6.9	94.6	39.1	138.2	100.0
May	27.6	26.5	13.1	11.2	101.7	16.9	165.7	177.0
June	30.1	29.9	12.6	13.5	46.0	0.3	220.4	233.1
July	31.8	32.8	13.8	13.9	1.0	0.6	270.2	281.1
August	31.7	32.7	14.9	15.0	7.8	3.9	220.0	245.0
September	30.7	30.3	13.7	14.9	49.7	41.5	164.3	184.8
October	28.1	23.3	122	11.4	44.8	95.1	139.7	101.9
November	17.7	16.6	8.5	7.9	141.1	227.6	50.5	39.5
December	15.4	15.9	4.3	6.5	12.5	61.6	36.4	33.1

During the study period (years 2011 and 2012), irrigation was applied almost every day during the spring and summer periods. A drip irrigation system with spacing of 0.75 m between emitters and an emitter discharge of 2.3 l h^{-1} was used. The fraction of ground area wetted by irrigation was $f_w = 0.23$.

In 2012, between February 20th and 25th, an extremely heavy frost affected the orchard, causing a strong leaf fall. A severe pruning of the trees was therefore applied following the frost occurrence. Some areas of the olive orchard were more affected by the frost, and consequently the pruning was not uniform along the orchard, which increased the variability of the vegetation conditions within the orchard in 2012.

2.2. Field data

Data obtained from ground-based measurements were used to validate information of several agronomic and biophysical parameters computed from METRIC. A short description of the measurements performed is presented herein; further information can be found in Paço et al. (submitted for publication). The soil evaporation (E_s) was measured in both years during summer ($n = 8$) with a set of six microlysimeters following Daamen, Simmonds, Wallace, Laryea, and Sivakumar (1993). Microlysimeters were distributed in three representative areas considering soil exposure to solar radiation and surface wetness by irrigation. The Granier (1985) method was used for sap-flow measurements to obtain plant transpiration (T_{sf}) data, using a set of 6 sensors (1 cm length, UP GmbH, Germany). Measurements were collected between DOY (day of year) 134/2011 and 366/2012, with 30-min data being stored in a datalogger (Model CR1000, Campbell Scientific, Inc., Logan, UT, USA).

Crop evapotranspiration was assessed by eddy covariance (EC) measurements (ET_{ec}) performed with a 3D sonic anemometer and a krypton hygrometer (Models CSAT3 and KH20, Campbell Scientific, Inc., Logan, UT, USA) connected to a datalogger (Model CR1000, Campbell Scientific, Inc., Logan, UT, USA). The sensors were placed on a metallic tower, located near the centre of the orchard, at a measurement height of 4.8 m. Raw data for sensible heat flux density (H) and latent heat flux density (λE) were collected at a 10 Hz frequency during 13 days in July–August 2011 and during 28 days in June–August 2012. Data were further analysed with the Software package TK3 (University of Bayreuth, Germany), corrected following Foken, Leuning, Oncley, Mauder, and Aubinet (2011) and submitted to a coordinate rotation (Kaimal & Finnigan, 1994). Eight soil heat flux plates (calibrated Peltier modules sealed 20 V, 4.4 A, 40 × 40 × 3.9 mm, RS Components, Madrid, Spain) distributed by the tree row and between the rows were placed at a depth of 2 cm to measure the soil heat flux (G). The net radiation (R_n) was measured with a net radiometer (Model, NR-LITE, Kipp and Zonen, Delft, NL). Further information on ground-based observations is given by Paço et al. (submitted for publication).

The data series collected with the EC technique were related with sap-flow data as detailed by Paço et al. (submitted for publication). Soil evaporation data were simulated using Ritchie's model (Ritchie, 1972) within the SIMDualKc model suite (Rosa et al., 2012) as analysed by Paço et al. (submitted for publication). Daily observed ET data (ET_{obs}) were derived from sap-flow calibrated data (T_{sf}) and soil evaporation simulated via SIMDualKc ($E_{s\ sim}$): $ET_{obs} = T_{sf} + E_{s\ sim}$ [mm d^{-1}], as described by Paço et al. (submitted for publication).

Temperatures of shaded soil surface and sunlit soil surface were measured with infrared sensors (Apogee, Model SI-111) and the hourly average data were recorded in a datalogger (Campbell Scientific, Inc., Logan, UT, USA). Data for the shaded soil surface were collected from May to October in 2011, while data for a sunlit soil surface were collected from June to October, both in 2011 and 2012. Temperatures of the canopy were continuously recorded by an infrared sensor placed above the canopy, from July 2011 until the end of 2012. Additionally, an infrared camera (ThermCam Model SC640, FLIR systems) was used to obtain thermal-infrared images of 30 trees distributed through the olive orchard at several dates. Thermal-infrared images were captured at side-view, considering an orientation Southeast–Northeast. The difference between the average value of the temperatures recorded by the infrared camera for the 30 trees on specific dates and the value recorded with the infrared sensor was used to adjust the canopy temperatures to values representative of all the orchard trees. The ground-based temperatures were used for comparison with values estimated in METRIC for the temperatures of the canopy (T_c), of the shaded ground surface (T_{shadow}), and of the sunlit ground surface (T_{sunlit}). For this comparison, the mean absolute differences and the mean bias were computed. The mean absolute difference was computed as the absolute value for the difference between the average temperature estimated with METRIC for the full set of pixels in the study area (T_{METRIC}) and the ground-based temperature measured in the field ($T_{ground\ data}$), for each specific date. The mean bias was computed as $(T_{METRIC} - T_{ground\ data})/T_{ground\ data}$.

A set of eight Quantum sensors (QPAR-02, 400–700 nm, Tranzflo, Palmerston, NZ) placed in a fixed grid around the trees and one at the top of the canopy were used to measure the photosynthetically active radiation (PAR) and further derive leaf area index (LAI). The LAI was indirectly estimated based on the light interception measurements and using the Beer–Lambert law by considering the expression (Marshall & Waring, 1986):

$$LAI = [-\ln(Q_i/Q_0)]/K \quad (1)$$

where Q_i [μmol m^{-2}] corresponds to daily PAR measured at the top of the canopy, Q_0 [μmol m^{-2}] is the daily PAR measured below the canopy and K is the extinction coefficient, that was set to 0.6 based on the olive tree study reported by Zarco-Tejada, Miller, Morales, Berjón, and Agüera (2004).

Meteorological data used in the METRIC application came from a reference weather station located close to the study area (Latitude 38° 21′ 42″ N, longitude 08° 07′ 29″ W, and elevation 138 m). A quality control of the weather data was applied following the procedures recommended by Allen et al. (1998) and ASCE-EWRI (2005). Hourly wind speed, air temperature (maximum and minimum), solar radiation, and relative humidity data were used to estimate the alfalfa reference evapotranspiration (ET_r) (ASCE-EWRI, 2005) using the software REF-ET (Allen, 2012). Daily precipitation data were used to perform a soil water balance of the upper soil layer for the

days preceding the satellite overpass, following the procedure proposed in FAO 56 Guidelines (Allen et al., 1998) aiming to assess ET for bare soil conditions.

2.3. Satellite data and ancillary data

Several satellite images from sensors Landsat 5 TM and Landsat 7 ETM+ (path203/row033) were used in the application of the METRIC algorithm, as detailed in Table 2. The images had L1T processing level, i.e., with geometric and terrain correction. All the satellite images were cloud-free over the selected study area.

A digital elevation model was used to correct the surface temperature according to the differences in elevation and to produce slope and aspect maps required in METRIC to estimate solar radiation (Allen, Trezza, & Tasumi, 2006). A land cover map obtained from CORINE Land Cover 2006 (scale 1:100,000) was used to support the estimation of the momentum roughness length, which was used to calculate convective heat transfer.

3. Surface energy balance and adaptations of METRIC algorithm for woody canopies

METRIC is based upon the energy balance at the land surface, thus computing the latent heat flux (λE) by subtracting soil heat flux (G) and sensible heat flux (H) from net radiation (R_n), with all units in [W m^{-2}]

$$\lambda E = R_n - G - H \quad (2)$$

The latent heat flux is computed for each pixel at the instant of satellite overpass and is readily converted to instantaneous ET (Allen, Tasumi, & Trezza, 2007)

$$ET_{inst} = 3600\ \lambda E/\lambda \quad (3)$$

where ET_{inst} is the instantaneous ET [mm h^{-1}], 3600 is the time conversion from seconds to hours, λE is the latent heat flux [W m^{-2}], and λ is the latent heat of vaporisation [J kg^{-1}].

The fraction ETrF, which can also be termed an alfalfa-reference-based crop coefficient, K_{cr} (Allen, Pereira, Howell, & Jensen, 2011), is the ratio of the instantaneous ET derived for each pixel to the alfalfa reference ET_r. ETrF was computed for the time of the satellite overpass, thus $ETrF_{inst} = ET_{inst}/ET_r$. The tall alfalfa reference ET_r is used in METRIC calibration and time-based interpolation because ET_r represents a near maximum limit on ET from full-cover vegetation. Values for ET_r average about 1.2–1.4 times greater than the shorter clipped grass reference ET_o (ASCE-EWRI, 2005). The $ETrF_{inst}$ is commonly used to translate ET_{inst} to longer periods such as the day, assuming that the $ETrF_{inst}$ is the same as the 24 h average ETrF. This assumption has been shown to be valid for agricultural crops developed to maximise photosynthesis and stomatal conductance (Allen, Irmak et al., 2011). However, differently from other agricultural crops, olive trees show an important stomatal control, closing stomata under conditions of high evaporative demand and having stomata wider open in the morning relative to the afternoon (e.g., Fernández, Moreno, Girón, & Blázquez, 1997; Moriana, Villalobos, & Fereres, 2002; Ramos & Santos, 2009). Moreover, as analysed with the model SIMDualKc (Paço et al., submitted for publication), the olive orchard was under mild to moderate water stress during limited summer periods, which may have led to a decrease in ETrF during the part of the day when vapour pressure deficit values were higher. It therefore becomes necessary to adjust the scaling coefficient ETrF during the mid-season period in a way similar to that reported by for the grass-based crop coefficients, K_c. Hence, in the mid-season period, when the daily average temperatures were higher (>20 °C) and maximum relative humidity was lower (≤70%), thus when the vapour pressure deficit was higher, the translation of ET_{inst} into daily ET was based on an evaporation fraction, EF. This EF is computed as the ratio between ET_{inst} and the difference $R_n - G$, thus $EF = ET_{inst}/(R_n - G)$ (Allen, Pereira et al., 2011). The use of EF for the satellite images of the mid-season period provided an adjustment for daily actual ET and daily ETrF.

In the application of METRIC algorithm, two "anchor points for calibration" – the "cold pixel" and the "hot pixel" – are selected to define the limit conditions for the energy balance over the study area. The cold pixel is selected and defined over a well irrigated and non-stressed cropped field, representing maximum ET (with ET set to $ET_{cold\ pixel} = 1.05\ ET_r$), while the hot pixel is selected and defined over a bare agricultural soil (Allen, Tasumi, & Trezza, 2007). A daily soil water balance of the surface layer was used to estimate $H = R_n - G - ET_{bare\ soil}$ for the hot pixel (Allen, Tasumi, & Trezza, 2007).

In the application of the single-layer METRIC algorithm to sparse woody canopies as olive orchards, some extensions related with the estimation of vegetation temperature and of momentum roughness length for tall vegetation, which may impact the estimation of the sensible heat flux, were considered and assessed.

In METRIC, the estimation of sensible heat flux is a function of the temperature gradient above the surface (dT), which is approximated through a simple linear function of the radiometric surface temperature, T_s (Bastiaanssen et al., 1998). It is also a function of the aerodynamic resistance to heat transport between two heights ($r_{ah1,2}$), which is computed using the extrapolation of wind speed from some blending height above the surface and an iterative stability correction scheme based on the Monin and Obukhov (1954) equations. Additionally, the computation of H considers wind speed and the surface roughness. The latter is estimated according to the land cover type or amount of vegetation (Allen, Tasumi, & Trezza, 2007).

Table 2 – Summary of the satellite image dates used for the METRIC application.

Sensor	Dates (DOY)	Sensor	Dates (DOY)
Landsat 5 TM	31 January 2011 (31) 20 March 2011 (79) 5 April 2011 (95) 23 May 2011 (143) 24 June 2011 (175) 26 July 2011 (207) 27 August 2011 (239) 12 September 2011 (255) 6 October 2011 (279) 30 October 2011 (303)	Landsat 7 ETM+	11 February 2012 (42) 15 April 2012 (106) 20 July 2012 (202) 21 August 2012 (234) 6 September 2012 (250)

In the application of the algorithm, both dT and $r_{ah1,2}$ are estimated in a blended zone above the vegetation canopy where effects from underlying vegetation and soil surface are combined to fit similar blending presented by the satellite. Thus, this blending zone is assumed to be sufficiently mixed regarding the blend of vegetation and soil, so that a single dT can be formulated to describe the blend of localised dT within a satellite pixel (Allen, Pereira et al., 2011). The bulk values for T_s derived from thermal pixels in Landsat images (60–120 m) tend to correlate with the blended dT, thus allowing adequate estimates of ET for olive orchards (Santos et al., 2012).

In recent applications of METRIC to tall vegetation, such as in orchards and forests, the estimation of Z_{om} is based on a Perrier (1982) equation, as described in Allen, Irmak et al. (2011), Allen et al. (2012). Alternatively, Z_{om} can assume a constant value within the range of values proposed by Allen et al. (2012). The Perrier equation is written as

$$Z_{om} = \{[1 - \exp(-a\,\mathrm{LAI}/2)]\exp(-a\,\mathrm{LAI}/2)\}h \quad (4)$$

where h [m] is the crop height, LAI is the leaf area index [$m^2\ m^{-2}$], and a is an adjustment factor for LAI distribution within the canopy with $a = (2f_{LAI})$ for $f_{LAI} \geq 0.5$ and $a = [2(1 - f_{LAI})]^{-1}$ for $f_{LAI} < 0.5$. The factor f_{LAI} is the proportion of LAI lying above $h/2$, which was set to 0.6 considering the architecture of the olive trees in the studied orchard.

LAI is conventionally computed in METRIC using the soil adjusted vegetation index (SAVI) and h (Allen, Tasumi, & Trezza, 2007; Allen et al., 2012). However, as the traditional equation used in METRIC underestimated the LAI values for the studied olives orchard, an adjustment for the computation of this parameter was necessary. The LAI estimates were adjusted according to information collected in the field and SAVI data, and considering LAI values obtained by Diaz-Espejo et al. (2012) for a hedgerow olive orchard whose characteristics are similar to those of the study area

$$\mathrm{LAI}_{j,i} = \mathrm{LAI}_{max}\left[\left(\mathrm{SAVI}_{j,i} - \mathrm{SAVI}_{min,i}\right)/\left(\mathrm{SAVI}_{max,i} - \mathrm{SAVI}_{min,i}\right)\right] + 0.01 \quad (5)$$

where $\mathrm{LAI}_{i,j}$ is the LAI for each pixel and date, LAI_{max} is the maximum LAI based on Diaz-Espejo et al. (2012) values obtained in specific periods of the year for a fully irrigated hedgerow olive orchard, $\mathrm{SAVI}_{i,j}$ is the SAVI for each pixel and date, and $\mathrm{SAVI}_{min,j}$ and $\mathrm{SAVI}_{max,j}$ are respectively the minimum and maximum values of SAVI in each date for the olive orchard under study. The equation (5) for LAI computation was specifically adjusted for the olive orchard under study. Following this adjustment, and considering the crop height data collected in the field, the relationship $h = 3.5\mathrm{LAI}$ was obtained for the olives orchard under study, to provide estimates of tree height for average field observations.

As previously mentioned, in tall and discontinuous vegetation, the surface temperature observed by a satellite integrates a mixture of the temperatures of sunlit and shaded canopy surfaces, along with sunlit and shaded soil surfaces, which are often different from each other. Therefore, the computation of the radiometric surface temperature T_s for discontinuous woody crops such as olive orchards can be expressed as (Allen & Kjaersgaard, 2009)

$$T_s = f_c T_c + f_{shadow} T_{shadow} + f_{sunlit} T_{sunlit} \quad (6)$$

where f_c, f_{shadow} and f_{sunlit} are respectively the relative fraction of ground covered by the vegetation, and shadow and sunlit ground surface when viewed from nadir, so that $f_c + f_{shadow} + f_{sunlit} = 1$, and T_c, T_{shadow} and T_{sunlit} are the temperature of the canopy, of the shaded ground surface and of the sunlit ground surface, respectively. As the sunlit canopies are the primary source of energy exchange in tall canopies such as trees, the effective temperature for tall canopies can be better adjusted if estimated by solving equation (6) for T_c. Thus, the canopy temperature, which is then used in the METRIC 'dT' function for sensible heat flux calculation, is estimated as

$$T_c = \left(T_s - f_{shadow} T_{shadow} - f_{sunlit} T_{sunlit}\right)/f_c \quad (7)$$

T_{shadow} and T_{sunlit} are estimated as (Allen & Kjaersgaard, 2009)

$$T_{shadow} = T_{coldpixel} - \left(T_{coldpixel} - T_{wetbulb}\right)/K_{shadow} \quad (8)$$

$$T_{sunlit} = T_{coldpixel} + \left(T_{hotpixel} - T_{coldpixel}\right)/K_{sunlit} \quad (9)$$

where $T_{hotpixel}$ and $T_{coldpixel}$ are the temperatures of the hot and cold pixels, and $T_{wetbulb}$ is the wet bulb temperature estimated from air temperature and relative humidity, K_{shadow} is a fitting coefficient ranging between 1 and 5, and K_{sunlit} is a fitting coefficient ranging from 1 to 4. A value of 3 was used both for K_{shadow} and K_{sunlit} based on field data information. Rationale for the form and parameters used in equations (8) and (9) is provided in Allen and Kjaersgaard (2009).

The f_c fraction of ground cover by vegetation (see equations (6) and (7)) was estimated from the Normalised Difference Vegetation Index (NDVI) data. For our olive orchard, taking into consideration field observations for f_c, it was defined as

$$f_c = 0.59(\mathrm{NDVI}_i - \mathrm{NDVI}_{min})/(\mathrm{NDVI}_{max} - \mathrm{NDVI}_{min}) + 0.01 \quad (10)$$

where NDVI_i is the NDVI for each pixel, and NDVI_{min} and NDVI_{max} are respectively the average minimum and maximum values of NDVI for a super-intensive olive orchard. Based on the analysis of the NDVI results in the olive orchard for 15 image dates of 2011 and 2012, the values of NDVI_{min} and NDVI_{max} were set to 0.21 and 0.60, respectively. The parameters of equation (10) should be adjusted when applications concern different orchards.

The fraction of shaded ground was based upon the shadow visible from nadir and was estimated as (Allen & Kjaersgaard, 2009)

$$f_{shadow} = \min\left(1 - f_c, f_{stot} - f_c f_{nonvisible}\right) \quad (11)$$

where f_{stot} is the fractional area covered by a shadow cast by the crowns, $f_{nonvisible}$ is the fraction of the canopy that has a shadow under it and is not visible from the satellite because it is covered by the canopy, and f_{stot} and $f_{nonvisible}$ were estimated with the equations proposed respectively by Allen and Kjaersgaard (2009) and Campbell and Norman (1998)

$$f_{stot} = f_c/\cos(\theta) \quad (12)$$

$$f_{nonvisible} = 1 - \left(f_{shape}\left(h f_{bl}/\tan(\pi/2 - \theta)\right)\right)/w \quad (13)$$

where f_{shape} is a factor to adjust for differences in shape between trees and their shadow when viewed from nadir, h is the tree height, f_{bl} is a factor describing the proportion of bottom leafless portion of the tree and not casting a shadow due to the total height of the tree, θ is the sun zenith angle [rad], and w is the vegetation width [m] as described by Campbell and Norman (1998).

The fraction of the ground that receives direct solar radiation visible from nadir was estimated as (Allen & Kjaersgaard, 2009)

$$f_{sunlit} = \max(0, 1 - f_c - f_{shadow}) \quad (14)$$

Further details of METRIC algorithm are given by Allen, Tasumi, and Trezza (2007), Allen et al. (2012). The software ERDAS IMAGINE v.2010 (Leica Geosystems) was used for the application of METRIC algorithm.

4. Results and discussion

4.1. *Improvements in METRIC parameterisation relative to LAI, Z_{om} and T_s*

The results of LAI obtained with the equation conventionally used in the METRIC algorithm (LAI = 11SAVI^3) ranged between 0.46 and 0.75 m^2 m^{-2} in 2011 and between 0.33 and 0.68 m^2 m^{-2} in 2012. These values are higher than the results reported by Santos et al. (2012) for rainfed traditional olive orchards having lower tree density (70–200 trees ha^{-1}). In contrast, these LAI values are lower than those reported by Diaz-Espejo et al. (2012) for a hedgerow olive orchard with characteristics similar to the ones of the orchard under study. Those LAI values are also lower than the values estimated from field PAR measurements, and no correlation was found between the two datasets (data not shown).

Adopting equation (5) to compute LAI in the olive orchard under study led to improved estimation of this parameter in the METRIC algorithm. The new LAI results showed a good agreement between data estimated by METRIC and data estimated with PAR data. Comparing these data with a regression forced through the origin resulted a regression coefficient close to 1.0 ($b = 0.95$) and a R^2 of 0.81 (Fig. 2). The LAI estimated by the improved METRIC algorithm for hedgerow olives (equation (5)) ranged between 0.74 and 1.23 m^2 m^{-2} for the year 2011 and between 0.62 and 0.96 m^2 m^{-2} in 2012, with lower values occurring during winter and early spring. The lower LAI values for 2012 were due to the occurrence of a severe frost during winter that caused a strong leaf fall and made necessary an intense pruning of the trees. The results for 2011 are within the range of values presented by Diaz-Espejo et al. (2012).

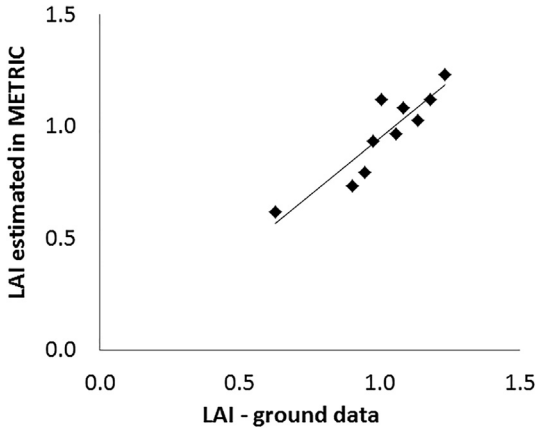

Fig. 2 – Comparing LAI computed with METRIC using equation (5) with LAI obtained from field PAR measurements (LAI–ground data) for 10 image dates between July 26th 2011 and September 6th 2012 ($y = 0.951x$; $R^2 = 0.813$; $n = 10$).

The estimation of Z_{om} may have an important impact on the performance of the METRIC algorithm applied to sparse woody canopies as it impacts the estimation of H. Therefore, following the adoption of improvements in Z_{om} derivation from METRIC as described in Section 3, Z_{om} computed with the Perrier equation (equation (4)) were compared with other Z_{om} values published in the literature for tree crops and olive orchards with different tree density (Allen et al., 2012; Berni, Zarco-Tejada, Sepulcre-Cantó, Fereres, & Villalobos, 2009; Santos et al., 2012; Villalobos, Orgaz, Testi, & Fereres, 2000).

The average Z_{om} from equation (4) was 0.81 m (ranging between 0.74 and 0.85 m) and the average Z_{om}/h ratio was 0.24 (ranging from 0.22 to 0.25), for the set of images considered. These results are similar to those reported by Allen et al. (2012) when applying the same equation for tree species with LAI similar to that observed in the studied olive orchard (Z_{om}/h values around 0.21–0.25). These results are higher than those presented in other studies where different parameterisations were used for the aerodynamic resistance, reporting values of 0.068–0.15 h for olive orchards with a lower number of trees, 70–280 trees ha^{-1} (Berni et al., 2009; Santos et al., 2012; Villalobos et al., 2000). Nevertheless, the higher values for the Z_{om} obtained in the current study relate to the higher density of the super-intensive olive orchard (1975 trees ha^{-1}) since, as discussed before, Z_{om} increases as the orchard density increases up to a threshold LAI of 3 m^2 m^{-2} (Allen et al., 2012).

The mean absolute difference between ground data and METRIC estimated data for T_{shadow} was 3.6 K, representing a mean bias of 1.23% (over six image dates), with mean differences ranging from −3.6 to 8.3 K. The mean absolute difference for the T_{sunlit} was 3.5 K, representing a mean bias of 1.13% (over eight image dates), with mean differences ranging between 1.6 and 6.8 K. Regarding T_c, the mean absolute difference between ground data and METRIC estimated data was 5.0 K, corresponding to a mean bias of 1.66% (over nine image dates), with mean difference values ranging from 0.3 to 9.3 K. Part of this bias may be due to the differences between satellite-based retrievals of surface temperature that were not corrected for atmospheric impacts and the ground-based observations. Moreover, using a regression through the origin to compare the temperature of the canopy estimated by METRIC with that obtained from field measurements resulted in a regression coefficient $b = 1.02$, thus very close to 1, and a high R^2 of 0.89 (Fig. 3).

Differences between the temperature of the soil (either shaded or sunlit) and of the canopy were up to 20 K (Fig. 4), which are similar to results reported by Sepulcre-Cantó et al. (2006). Larger differences were observed between T_{shadow}

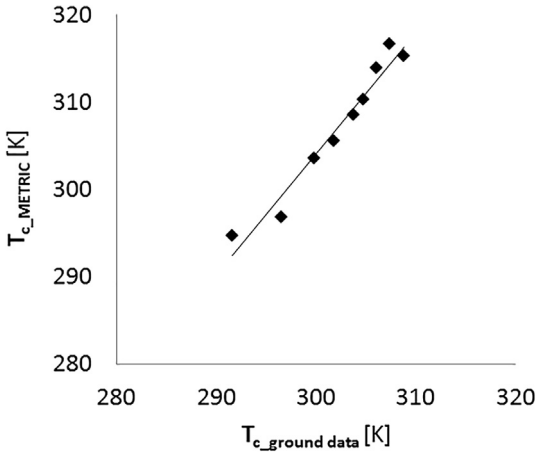

Fig. 3 – Comparing the temperature of the canopy (T_c) derived from METRIC (T_{c_METRIC}) with that obtained from ground data ($T_{c\_ground\ data}$) ($y = 1.017x$; $R^2 = 0.8876$; $n = 9$).

and T_c (Fig. 4). However, f_{shadow} (equation (6)) is the less representative component of the relative fractions of ground cover, except for the winter and mid to late autumn dates, when the differences between the various components of the temperatures (Fig. 4) were also small. Values of f_{shadow} ranged between 0.09 and 0.20 in the spring and summer, and between 0.26 and 0.54 in autumn and winter periods, thus in agreement with the sun angle at nadir.

For the dates of the spring and summer periods, the value of T_c was larger than T_{sunlit} (Fig. 4) because, at the time of satellite overpass, the f_{sunlit} integrates a mix of dry and wet soil due to irrigation.

4.2. *Performance of METRIC algorithm when applied to olive orchards*

To evaluate the performance of METRIC algorithm when applied to the olive orchard and following the adoption of improvements in the computation of Z_{om} and surface temperature, the results of ET estimated using those improvements were compared with results obtained using the approaches commonly applied in METRIC. For that comparison, we considered the mean differences between ET derived from METRIC (ET_{METRIC}, corresponding to the average of ET of the vegetated pixels in the olive orchard) and the ET obtained from ground data (ET_{obs}). Table 3 shows the mean differences between ET_{METRIC} and ET_{obs}, for ET_{METRIC} estimated: (i) by computing the surface temperature with the adjustment in equation (6) ($T_{s\ adj}$) or without that adjustment ($T_{s\ no\ adj}$), and (ii) by considering different options for the Z_{om} computation as suggested by Allen et al. (2012) for woody crops.

The comparison of the results related to the computation of Z_{om} showed that mean differences in the ET estimate do not differ much between the options considered (Table 3). The application of the Perrier equation showed good results for the ET estimation in the olive orchard under study (Table 3, $Z_{om} = f(LAI,h)$), with small differences when compared to the other options where Z_{om} was held constant (Table 3). For some dates, the mean differences $ET_{METRIC} - ET_{obs}$ were smaller when a constant value of Z_{om} was considered (Table 3). Nevertheless using the Perrier equation (equation (4)) provides for a Z_{om} that varies with LAI and h, therefore allowing the spatial variability of the vegetation conditions within the olive orchard to be considered. The average difference $ET_{METRIC} - ET_{obs}$ was 0.06 mm d^{-1} when comparing $Z_{om} = f(LAI,h)$ with $Z_{om} = 1.0$ m, was 0.01 mm d^{-1} when the comparison was made with $Z_{om} = 0.8$ m, and was -0.07 mm d^{-1} when comparing with $Z_{om} = 0.5$ m. Hence, for the set of dates considered, the differences $ET_{METRIC} - ET_{obs}$ are small.

The computation of Z_{om} with the Perrier equation in METRIC was previously tested with good results in rainfed traditional olives orchards (Santos et al., 2012), thus showing its adequacy for orchards having quite different characteristics. As discussed in Section 4.1, different Z_{om}/h ratios can be associated to orchards having different tree densities and canopy architectures, thus a constant Z_{om} might not be suitable for olive orchards with characteristics differing from those of the studied orchard because, contrarily to the use of equation (4), it does not adjust for tree density and architecture. Future research should verify whether the use of the Perrier equation is appropriate to other orchard types.

Regarding the sensitivity tests for the application of the three-source condition (equation (6)) for the computation of

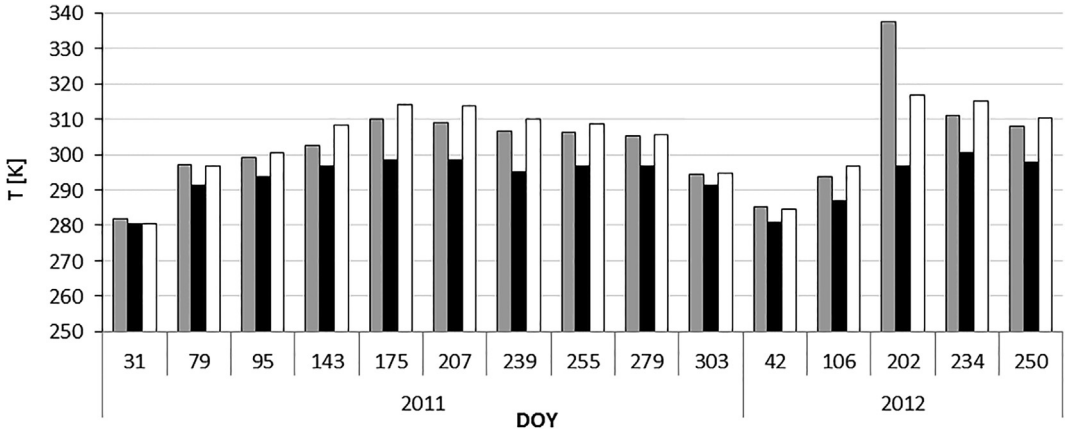

Fig. 4 – Daily average temperatures of the soil sunlit surface (■ T_{sunlit}), soil shaded surface (■ T_{shadow}), and canopy (□ T_c) computed from METRIC for the set of pixels of the olive orchard under study.

Table 3 – Mean difference ($ET_{METRIC} - ET_{obs}$) [mm d^{-1}] between evapotranspiration obtained from METRIC and from ground data considering different approaches in the computation of the momentum roughness length (Z_{om}) and of the surface temperature (T_s).

DOY (Year)	$Z_{om} = f(LAI,h)$[a]		Z_{om} = 1.0 m		Z_{om} = 0.8 m		Z_{om} = 0.5 m	
	$T_{s\ adj}$[b]	$T_{s\ no\ adj}$[c]	$T_{s\ adj}$	$T_{s\ no\ adj}$	$T_{s\ adj}$	$T_{s\ no\ adj}$	$T_{s\ adj}$	$T_{s\ no\ adj}$
143 (2011)	0.81	1.10	0.79	1.09	0.81	1.11	0.83	1.13
175 (2011)	0.38	1.20	0.29	1.12	0.38	1.20	0.54	1.33
207 (2011)	0.38	1.56	0.31	1.51	0.38	1.55	0.50	1.63
239 (2011)	−0.19	1.07	−0.23	1.05	−0.19	1.07	−0.11	1.10
255 (2011)	0.00	1.36	−0.02	1.36	0.01	1.36	0.05	1.36
279 (2011)	−0.76	0.35	−0.77	0.36	−0.76	0.35	−0.76	0.32
303 (2011)	0.41	1.37	0.40	1.38	0.41	1.37	0.42	1.34
42 (2012)	0.36	1.10	0.30	1.04	0.35	1.09	0.45	1.18
106 (2012)	0.13	0.97	−0.10	0.77	0.03	0.89	0.27	1.11
202 (2012)	1.24	2.41	1.15	2.37	1.21	2.40	1.32	2.46
234 (2012)	0.82	2.19	0.79	2.18	0.81	2.18	0.86	2.18
250 (2012)	0.53	1.91	0.50	1.90	0.53	1.91	0.58	1.91
Mean absolute difference	0.52	1.41	0.49	1.38	0.51	1.40	0.58	1.45
Mean difference	0.38	1.41	0.32	1.38	0.36	1.40	0.34	1.45

[a] Z_{om} computed with the Perrier equation (Eq. (4)).
[b] Surface temperature computed using the three-source condition (Eq. (6)), i.e., differentiating the temperatures of the canopy, of the shaded ground surface and of the sunlit ground surface.
[c] Surface temperature computed without considering the three-source condition.

radiometric surface temperature ($T_{s\ adj}$), the results in Table 3 have shown a better performance for the ET estimation for all Z_{om} computation options considered, as opposed to applying METRIC using the bulk T_s from satellite, only. When the equation (6) was not applied ($T_{s\ no\ adj}$), larger mean differences in $ET_{METRIC} - ET_{obs}$ were obtained, ranging between 0.3 and 2.5 mm d^{-1} when considering all dates and all options for Z_{om} computation (Table 3). These results show the importance of considering the three-source condition in the computation of surface temperature and, thus, in obtaining the temperature of the canopy, which was then used in the METRIC 'dT' function for sensible heat flux estimation. This approach is also a way of overcoming the limitations of one-source models relative to two-source models and it is likely applicable to other orchard types, which is a theme for future research.

4.3. *Evapotranspiration estimated with METRIC algorithm*

Following the results presented in the previous Sections, equations (4)–(6) for the computation of Z_{om}, LAI, and surface temperature were adopted in METRIC for the estimation of ET of the super-intensive olive orchard under study. The results of ET_{METRIC}, corresponding to the average of ET of the vegetated pixels in the olive orchard, thus excluding pixels of roads or buildings within the orchard, were compared against ET derived from ground data, ET_{obs} (as defined in Section 2.2).

ET_{METRIC} and ET_{obs} followed a similar pattern as shown in Fig. 5. The mean value for ET_{METRIC} in 2011 was 3.58 mm d^{-1}, with values ranging between 1.88 and 6.0 mm d^{-1} (Table 4), while the mean value for ET_{obs} was 3.44 mm d^{-1}, with values ranging from 2.29 to 5.19 mm d^{-1}. In 2012 the mean value for ET_{METRIC} was 2.75 mm d^{-1}, with values ranging between 0.92 and 4.46 mm d^{-1}, that compared well with ET_{obs}, whose mean was 2.37 mm d^{-1} and range was 0.56–3.22 mm d^{-1} (Table 4). The lower ET values in 2012 were due to the severe frost occurrence and subsequent heavy pruning, which impacted the vegetation conditions as previously discussed.

The regression forced through the origin used to compare ET_{METRIC} and ET_{obs} showed $R^2 = 0.85$ and a regression coefficient $b = 1.11$, thus indicating that METRIC tended to slightly overestimate ET relative to ground-based computations (Fig. 6). The mean absolute difference between ET_{METRIC} and ET_{obs} for the dates in 2011 was 0.4 mm d^{-1} (corresponding to a mean bias of 12.6%), with the largest mean difference of 0.81 mm d^{-1} on May 23rd, DOY 143 (Table 4). For 2012, the mean absolute difference was larger, 0.6 mm d^{-1} (mean bias of 31.2%) and the largest mean difference was 1.2 mm d^{-1} (July 20th, DOY 202; Table 4). The overestimation in 2012 relates to the referred change in canopy architecture due to a large loss of leaves following the heavy frost in winter that was followed by a reduction of the canopy size by pruning.

These changes in canopy architecture were not uniform through the orchard but largely varied spatially. Therefore, the standard deviation (SD) of ET_{METRIC} for the pixels of the olive orchard was larger in 2012 than in 2011: SD values ranged between 0.19 and 0.50 mm d^{-1} in 2011, while in 2012 ranged from 0.31 to 0.82 mm d^{-1}. The large mean differences between ET_{METRIC} and ET_{obs} in 2012 (Table 4) also relate to the fact that results from METRIC consisted of an average value relative to all pixels of the olive orchard while ground data corresponded to point values and local measurements, which incorporate the unavoidable uncertainties associated with sampling. These differences largely explain the tendency of METRIC to overestimate ET relative to ground-based computations.

The mean differences observed between ET_{METRIC} and ET_{obs} for both years (Table 3) may also be due to limitations of METRIC since it is a one-dimensional blended surface energy balance algorithm while discontinuous woody crops could, in theory, be better represented by a two-source or two-

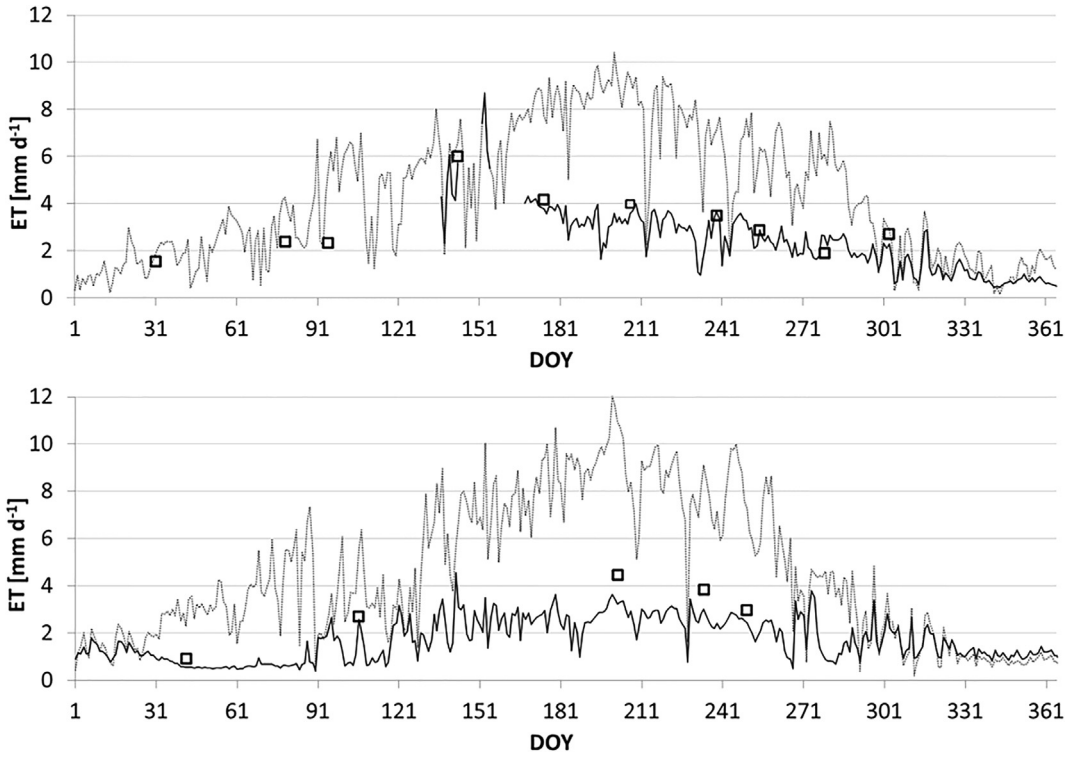

Fig. 5 – Evapotranspiration derived from ground data (––– ET_{obs}), ET derived from METRIC algorithm (□ ET_{METRIC}) and alfalfa reference evapotranspiration (——— ET_r) for 2011 (upper panel) and 2012 (lower panels).

dimensional model. Minacapilli et al. (2009) and Timmermans, Kustas, Anderson, and French (2007) reported that the two-source surface energy balance model TSEB performed slightly better in tree crops and sparse vegetation than one-source models because it is able to differentiate soil and vegetation components in the computation of the energy balance. However, the data required to parameterise and apply TSEB are often not readily available. Nevertheless, the use of a three-source condition in this study to compute surface temperature helped to overcome the limitation of the one-dimensional model; however, further research is needed.

The mean bias of 20% for the whole set of images integrates the effects of changes in canopy conditions in 2012 and would certainly be lower if these changes have not occurred, since in 2011 it was 12.6%. Nevertheless, it is within the range of values reported by Bastiaanssen et al. (2008) relative to the one-source model SEBAL applied to tree crops in various countries. That mean bias is also within the range of values

Table 4 – Evapotranspiration from field data (ET_{obs}) and computed with METRIC algorithm for the set of pixels of the olive orchard (ET_{METRIC}) and mean difference between ET_{METRIC} and ET_{obs}.

DOY (Year)	ET_{obs} [mm d^{-1}]	ET_{METRIC} [mm d^{-1}]	Mean difference [mm d^{-1}]
31 (2011)	–	1.54	–
79 (2011)	–	2.37	–
95 (2011)	–	2.33	–
143 (2011)	5.19	6.00	0.81
175 (2011)	3.79	4.17	0.38
207 (2011)	3.59	3.97	0.38
239 (2011)	3.68	3.49	−0.19
255 (2011)	2.87	2.87	0.00
279 (2011)	2.65	1.88	−0.76
303 (2011)	2.29	2.70	0.41
42 (2012)	0.56	0.92	0.36
106 (2012)	2.58	2.70	0.13
202 (2012)	3.22	4.46	1.24
234 (2012)	3.03	3.85	0.82
250 (2012)	2.46	2.99	0.53
Average	2.99	3.08	0.38
Mean absolute difference	–	–	0.52

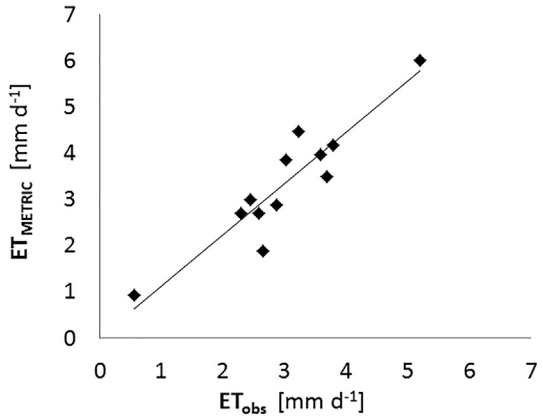

Fig. 6 – Comparing crop evapotranspiration derived from METRIC algorithm (ET_{METRIC}) and from ground data (ET_{obs}) ($y = 1.112x$; $R^2 = 0.8485$; $n = 12$).

presented by Allen, Tasumi, Morse et al. (2007) for the application of METRIC to several annual crops. Moreover, the observation and calibration of the field data have their own errors and uncertainties that may affect the computed bias.

5. Conclusions

The current application of the METRIC algorithm to estimate ET in a super-intensive olive orchard has shown good results when compared with ET derived from ground data. These positive results were possible because an appropriate parameterisation could be applied responding to the specific requirements of a dense hedgerow olive orchard. The innovative approaches to the METRIC application refer to (1) the adoption of a three-source condition for the computation of the radiometric surface temperature, (2) the computation of the momentum roughness length using the Perrier equation for Z_{om} estimation from the crop LAI and height, and (3) the adoption of a new equation to estimate LAI from SAVI. These approaches are expected to be applicable to different orchards and tree crops when appropriate parameterisation is adopted. Further testing with different discontinuous tree canopies is desirable. The ET from METRIC represents the average of the various pixels within the orchard which overcomes the sampling uncertainties relative to field observations. Differences between satellite and ground approaches are influenced by these conditions and by errors of METRIC parameterisation and errors of ground data observation and model calibration. Nevertheless, the results obtained were within the range of biases observed by other authors who have studied tree crops. Results from METRIC allowed the spatial variability of ET within the olive orchard to be understood. This allowed the consequences of defoliation following a heavy frost and the subsequent heavy pruning to be observed.

The results obtained with METRIC are appropriate for further estimation and mapping of evapotranspiration of olive orchards to support irrigation management mainly when associated with an irrigation scheduling simulation model. Nevertheless, further research must be implemented relative to olive orchards with different density and architecture characteristics, as well as for other tree and woody crops, so as to improve the parameterisation and use of METRIC algorithm.

Acknowledgements

This study was supported by European Regional Development Fund (ERDF), program COMPETE and National funds by FCT-Fundação para a Ciência e a Tecnologia, through the projects PTDC/AGR-PRO/111717/2009 and EXPL/AGR-PRO/1559/2012. The first author also acknowledges FCT for the Post-Doc research grant (SFRH/BPD/79767/2011). Developments of the METRIC processing algorithms were supported by Idaho Agricultural Experiment Station, Idaho Department of Water Resources, the US Geological Survey, NASA, the National Science Foundation EPSCoR program EPS-0814387, and Raytheon Company. Thanks are also due to Mr. António Nogueira for collecting ground data, Mr. Pedro Valverde for making available LAI data collected in the field, and Dr. Sofia Cerasoli for making available thermal-IR data recorded in the field.

REFERENCES

Allen, R. G. (2012). *REF-ET. Reference evapotranspiration calculator. (Version 3.1.08)*. Kimberly, Idaho: University of Idaho, Research and Extension Center.

Allen, R. G., & Kjaersgaard, J. (2009). *An algorithm to estimate vegetation temperature in canopies for tall vegetation*. Interoffice memo, Idaho: University of Idaho.

Allen, R., Irmak, A., Trezza, R., Hendrickx, J. M. H., Bastiaanssen, W., & Kjaersgaard, J. (2011). Satellite-based ET estimation in agriculture using SEBAL and METRIC. *Hydrological Processes, 25*, 4011–4027.

Allen, R. G., Pereira, L. S., Howell, T. A., & Jensen, M. E. (2011). Evapotranspiration information reporting: I. Factors governing measurement accuracy. *Agricultural Water Management, 98*, 899–920.

Allen, R. G., Pereira, L. S., Raes, D., & Smith, M. (, 1998). *Crop evapotranspiration: Guidelines for computing crop water requirements*. FAO Irrigation and drainage paper 56, Rome, Italy: FAO – Food and Agriculture Organization of the United Nations.

Allen, R. G., Tasumi, M., Morse, A., Trezza, R., Wright, J. L., Bastiaanssen, W., et al. (2007). Satellite-based energy balance for mapping evapotranspiration with internalized calibration (METRIC) – applications. *Journal of Irrigation and Drainage Engineering, 133*, 395–406.

Allen, R. G., Tasumi, M., & Trezza, R. (2007). Satellite-based energy balance for mapping evapotranspiration with internalized calibration (METRIC) – model. *Journal of Irrigation and Drainage Engineering, 133*, 380–394.

Allen, R. G., Trezza, R., & Tasumi, M. (2006). Analytical integrated functions for daily solar radiation on slopes for use in energy balance and evapotranspiration studies. *Agricultural and Forest Meteorology, 139*, 55–73.

Allen, R. G., Trezza, R., Tasumi, M., & Kjaersgaard, J. (2012). *METRIC™. Mapping evapotranspiration at high resolution. Applications manual for Landsat satellite imagery. Version 2.0.8*. Kimberly, Idaho: University of Idaho.

Anderson, M. C., Allen, R. G., Morse, A., & Kustas, W. P. (2012). Use of Landsat thermal imagery in monitoring evapotranspiration and managing water resources. *Remote Sensing of Environment, 122*, 50–65.

Anderson, M. C., Kustas, W. P., & Norman, J. M. (2003). Upscaling and downscaling – a regional view of the soil-plant-atmosphere continuum. *Agronomy Journal, 95*, 1408–1423.

ASCE. (1996). *Evaporation and transpiration, Hydrology handbook* (2nd ed.). New York: American Society of Civil Engineering.

ASCE-EWRI. (2005). In R. G. Allen, I. A. Walter, R. L. Elliott, T. A. Howell, D. Itenfisu, M. E. Jensen, et al. (Eds.), *The ASCE standardized reference evapotranspiration equation*. New York: ASCE-American Society of Civil Engineers.

Bastiaanssen, W. G. M., Menenti, M., Feddes, R. A., & Holtslag, A. A. M. (1998). A remote sensing surface energy balance algorithm for land (SEBAL). 1. Formulation. *Journal of Hydrology, 212–213*, 198–212.

Bastiaanssen, W. G. M., Pelgrum, H., Soppe, R. W. O., Allen, R. G., Thoreson, B. P., & Teixeira, A. H. C. (2008). Thermal infrared technology for local and regional scale irrigation analysis in horticultural systems. *Acta Horticulturae, 792*, 33–46. Vth IS on Irrigation of Horticultural Crops ISHS.

Berni, J. A. J., Zarco-Tejada, P. J., Sepulcre-Cantó, G., Fereres, E., & Villalobos, F. (2009). Mapping canopy conductance and CWSI

in olive orchards using high resolution thermal remote sensing imagery. *Remote Sensing of Environment, 113*, 2380–2388.
Calera, A., Jochum, A. M., García, A. C., Rodríguez, A. M., & Fuster, P. L. (2005). Irrigation management from space: towards user-friendly products. *Irrigation and Drainage Systems, 19*, 337–353.
Campbell, G. S., & Norman, J. M. (1998). *An introduction to environmental biophysics* (2nd ed.). New York: Springer-Verlag New York, Inc.
Campos, I., Neale, C. M. U., Calera, A., Balbontín, C., & González-Piqueras, J. (2010). Assessing satellite-based basal crop coefficients for irrigated grapes (*Vitis vinifera* L.). *Agricultural Water Management, 98*, 45–54.
Daamen, C. C., Simmonds, J. S., Wallace, J. S., Laryea, K. B., & Sivakumar, M. V. K. (1993). Use of microlysimeters to measure evaporation from sandy soils. *Agricultural and Forest Meteorology, 65*, 159–173.
Diaz-Espejo, A., Buckley, T. N., Sperry, J. S., Cuevas, M. V., de Cires, A., Elsayed-Farag, S., et al. (2012). Steps toward an improvement in process-based models of water use by fruit trees: a case study in olive. *Agricultural Water Management, 114*, 37–49.
D'Urso, G., Richter, K., Calera, A., Osann, M. A., Escadafal, R., Garatuza-Payan, J., et al. (2010). Earth Observation products for operational irrigation management in the context of the PLEIADeS project. *Agricultural Water Management, 98*, 271–282.
Fernández, J. E., Moreno, F., Girón, I. F., & Blázquez, O. M. (1997). Stomatal control of water use in olive tree leaves. *Plant and Soil, 190*, 179–192.
Foken, T., Leuning, R., Oncley, S. P., Mauder, M., & Aubinet, M. (2011). Corrections and data quality. In M. Aubinet, T. Vesala, & D. Papale (Eds.), *Eddy covariance: A practical guide to measurement and data analysis*. Berlin, Heidelberg: Springer.
Garatuza-Payan, J., & Watts, C. (2005). The use of remote sensing for estimating ET of irrigated wheat and cotton in Northwest Mexico. *Irrigation and Drainage Systems, 19*, 301–320.
Granier, A. (1985). Une nouvelle méthode pour la mesure du flux de sève brute dans le tronc des arbres. *Annales des Sciences Forestières, 42*, 193–200.
Heilman, J. L., Heilman, W. E., & Moore, D. G. (1982). Evaluating the crop coefficient using spectral reflectance. *Agronomy Journal, 74*, 967–971.
Jayanthi, H., Neale, C. M. U., & Wright, J. L. (2007). Development and validation of canopy reflectance-based crop coefficient for potato. *Agricultural Water Management, 88*, 235–246.
Kaimal, J. C., & Finnigan, J. J. (1994). *Atmospheric boundary layer flows: Their structure and measurement*. New York: Oxford University Press.
Kustas, W. P., Norman, J. M., Schmugge, T. J., & Anderson, M. C. (2004). Mapping surface energy fluxes with radiometric temperature. In D. Quattrochi, & J. Luvall (Eds.), *Thermal remote sensing in land surface processes* (pp. 205–253). Florida, USA: CRC Press Boca Raton.
McKnight, T. L., & Hess, D. (2000). *Climate zones and types: The Köppen system, physical geography: A landscape appreciation*. Upper Saddle River, NJ: Prentice Hall.
Marshall, J. D., & Waring, R. H. (1986). Comparison of methods of estimating leaf-area index in old-growth Douglas-fir. *Ecology, 67*, 975–979.
Minacapilli, M., Agnese, C., Blanda, F., Cammalleri, C., Ciraolo, G., D'Urso, G., et al. (2009). Estimation of actual evapotranspiration of Mediterranean perennial crops by means of remote-sensing based surface energy balance models. *Hydrology and Earth System Science, 13*, 1061–1074.
Monin, A., & Obukhov, A. (1954). Basic laws of turbulent mixing in the ground layer of the atmosphere. *Geofizicheskĭ Institut: Trudy, Akademiia Nauk SSSR, 151*, 163–187.
Moriana, A., Villalobos, F. J., & Fereres, E. (2002). Stomatal and photosynthetic responses of olive (*Olea europaea*) leaves to water deficits. *Plant, Cell and Environment, 25*, 395–405.
Orgaz, F., Testi, L., Villalobos, F. J., & Fereres, E. (2006). Water requirements of olive orchards. II: Determination of crop coefficients for irrigation scheduling. *Irrigation Science, 24*, 77–84.
Paço, T. A., Pôças, I., Cunha, M., Silvestre, J., Santos, F. L., Paredes, P., et al. Evapotranspiration and crop coefficients for a super intensive olive grove. An application of SIMDualKc and METRIC models using ground and satellite observations. *Journal of Hydrology*, submitted for publication.
Perrier, A. (1982). Land surface processes: vegetation. In P. Eagleson (Ed.), *Land surface processes in atmospheric general circulation models* (pp. 395–448). Cambridge University Press.
Pôças, I., Cunha, M., Pereira, L. S., & Allen, R. G. (2013). Using remote sensing energy balance and evapotranspiration to characterize Montane landscape vegetation with focus on grass and pasture lands. *International Journal of Applied Earth Observation and Geoinformation, 21*, 159–172.
Ramos, A. F., & Santos, F. L. (2009). Water use, transpiration, and crop coefficients for olives (cv. Cordovil), grown in orchards in Southern Portugal. *Biosystems Engineering, 102*, 321–333.
Ritchie, J. (1972). Model for predicting evaporation from a row crop with incomplete cover. *Water Resources Research, 8*, 1204–1213.
Rosa, R. D., Paredes, P., Rodrigues, G. C., Alves, I., Fernando, R. M., Pereira, L. S., et al. (2012). Implementing the dual crop coefficient approach in interactive software. 1. Background and computational strategy. *Agricultural Water Management, 103*, 8–24.
Santos, C., Lorite, I. J., Allen, R. G., & Tasumi, M. (2012). Aerodynamic parameterization of the satellite-based energy balance (METRIC) model for ET estimation in rainfed olive orchards of Andalusia, Spain. *Water Resources Management, 26*, 3267–3283.
Sepulcre-Cantó, G., Zarco-Tejada, P. J., Jiménez-Muños, J. C., Sobrino, J. A., Miguel, E.d., & Villalobos, F. J. (2006). Detection of water stress in olive orchard with thermal remote sensing imagery. *Agricultural and Forest Meteorology, 136*, 31–44.
Tasumi, M., & Allen, R. G. (2007). Satellite-based ET mapping to assess variation in ET with timing of crop development. *Agricultural Water Management, 88*, 54–62.
Testi, L., Villalobos, F. J., & Orgaz, F. (2004). Evapotranspiration of a young irrigated olive orchard in southern Spain. *Agricultural and Forest Meteorology, 121*, 1–18.
Testi, L., Villalobos, F. J., Orgaz, F., & Fereres, E. (2006). Water requirements of olive orchards: I simulation of daily evapotranspiration for scenario analysis. *Irrigation Science, 24*, 69–76.
Timmermans, W. J., Kustas, W. P., Anderson, M. C., & French, A. N. (2007). An intercomparison of the Surface Energy Balance Algorithm for Land (SEBAL) and the Two-Source Energy Balance (TSEB) modeling schemes. *Remote Sensing of Environment, 108*, 369–384.
Villalobos, F. J., Orgaz, F., Testi, L., & Fereres, E. (2000). Measurement and modeling of evapotranspiration of olive (*Olea europaea* L.) orchards. *European Journal of Agronomy, 13*, 155–163.
Zarco-Tejada, P. J., Miller, J. R., Morales, A., Berjón, A., & Agüera, J. (2004). Hyperspectral indices and model simulation for chlorophyll estimation in open-canopy tree crops. *Remote Sensing of Environment, 90*, 463–476.